International Journal of Control

ISSN: 0020-7179 (Print) 1366-5820 (Online) Journal homepage: http://www.tandfonline.com/loi/tcon20

PD-like controller for delayed bilateral teleoperation of wheeled robots

E. Slawiñski, V. Mut & D. Santiago

To cite this article: E. Slawiñski, V. Mut & D. Santiago (2016): PD-like controller for delayed bilateral teleoperation of wheeled robots, International Journal of Control, DOI: 10.1080/00207179.2016.1144234

To link to this article: http://dx.doi.org/10.1080/00207179.2016.1144234

Accepted author version posted online: 27 Jan 2016.

Publisher: Taylor & Francis
Journal: *International Journal of Control*
DOI: http://dx.doi.org/10.1080/00207179.2016.1144234

PD-like controller for delayed bilateral teleoperation of wheeled robots

E. Slawiñski*, V. Mut and D. Santiago

Instituto de Automática (INAUT). Universidad Nacional de San Juan. Av. Libertador San Martín 1109 (oeste). J5400ARL. San Juan, Argentina

**Corresponding author e-mail: slawinski@inaut.unsj.edu.ar*

Abstract—**This paper proposes a PD-like controller applied to the delayed bilateral teleoperation of wheeled robots with force feedback in face of asymmetric and varying-time delays. In contrast to bilateral teleoperation of manipulator robots, in these systems there is a mismatch between the models of the master and slave (mobile robot), problem that is approached in this work, where the system stability is analyzed. From this study, it is possible to infer the control parameters, depending on the time delay, necessary to assure stability. Finally, the performance of the delayed teleoperation system is evaluated through tests where a human operator drives a 3D simulator as well as a mobile robot for pushing objects.**

***Index Terms*—bilateral teleoperation, force feedback, PD-like controller, time delay, wheeled dynamic robot.**

I. INTRODUCTION

ROBOT teleoperation allows the execution of different tasks in remote environments including possibly dangerous and harmful jobs for the human operator [8]. In the teleoperation systems of robots with force feedback, a user completes some task physically interacting with the environment through a master-slave system. There are many applications for robot teleoperation, including telemedicine, exploration, entertainment, tele-services, tele-manufacturing and many more [17]. Additionally the use of the Internet as a communication channel increases the applications of the teleoperation systems. However, the presence of time-delays can induce instability or poor performance in a delayed teleoperation system [2], [7], [9] as well as a poor transparency [20].

There are many control schemes for standard teleoperation between two manipulators with time delay [2]. Within the proposed strategies, the concept commonly used inside the design of control schemes for bilateral teleoperation is the injection of damping into the system in order to assure its stability. For example, [1] proposed to send the scattering signals to transform the transmission delays into a passive transmission line. In [4] and [5], wave transformations are used to keep the passivity of the two-port channel in front of time delay. These strategies inject the so called apparent damping. In [16], a simple PD-like scheme, that does not require

scattering or wave variable transformations, yields a stable operation including the position coordination. From this, [6] and [18] proved asymptotic stability of PD-like schemes by using a sufficiently large damping injected into the master and slave for the case of constant delays and asymmetric time-varying delays, respectively. Recently, in [24] a reaction model of the human operator is included in order to decrease the necessary damping used to achieve stability. Other recent approaches like [26] consider linear both the master and slave in order to use the wide range of theoretical tools based on general LKF which are very useful for these delayed systems.

On the other hand, the state-of-the-art for delayed teleoperation of mobile robots is much less extensive. Some strategies involve: compensation based on a human operator model [10] but only visual feedback is considered, ordinary structures such as control based on impedance [19], event-based control [3], signals fusion [21], and other ones use only kinematic models like [11], [12], [13] and [14] , while [15] and [16] consider a dynamic model and analyze the r-passivity of the system. Recently, the concept of absolute transparency was proposed for bilateral teleleoperation of wheeled robots in order to analyze such feature [22]. One of the main reasons that rising the difficulty of applying many proposal existing in the current literature to mobile robot teleoperation, is caused by the mismatch between the models of the master and slave, for example if the master does not moves, the mobile robot generally goes at a constant speed.

This paper proposes a PD-like controller for the delayed bilateral teleoperation of wheeled robots, inspired in the controllers applied to bilateral teleoperation of manipulator robots like [18]. In our system, the human operator feels the mobile robot's dynamics through a force feedback in spite of the distance between the local and remote sites, providing the human operator a tactile perception of the task which improves his sense of telepresence. This work considers the dynamics of master and slave robots as well as time-varying and asymmetric delays. Furthermore, the controller is evaluated from two types of tests: first using a 3D simulator and second, teleoperating a mobile robot. In both cases, the human operator pushes an object through the master-slave (mobile robot) system. These experiences are made in order to verify the theoretical analysis achieved and evaluate the performance of the teleoperation system.

The paper is organized as follows: Section II presents some preliminary aspects such as the employed dynamic models, and the models used. In Section III a control scheme applied to bilateral teleoperation of unicycle-like wheeled robots is proposed. In addition, the stability analysis based on a Lyapunov-Krasovskii functional (LKF) is made. Sections V and VI show simulation and experimental results, where a user drives a wheeled robot. Finally, in section VII, the conclusions of this work are given.

II. PRELIMINARY

This paper will analyze teleoperation systems in which a human operator drives a wheeled robot while he feels the environment near the robot through visual and force feedback, as it is shown in Figure 1. For example the user could feel the weight of an object pushed by the mobile robot, which is remotely driven by a user through velocity commands generated by the master position.

Notation: We use standard notations throughout the paper. If x is a scalar, $\mathbf{y}$ is a vector and $\mathbf{Z}$ is a matrix, then $|x|$ is the absolute value of x, $\mathbf{y}^{\mathbf{T}}$ is the transpose $\mathbf{y}$, $\mathbf{Z}^{\mathbf{T}}$ is the transpose of the matrix, $|\mathbf{y}|$ is the Euclidean norm of $\mathbf{y}$, $|\mathbf{Z}|$ is the induced norm of $\mathbf{Z}$, $\mathbf{Z}>0$ ($\mathbf{Z}<0$) means that $\mathbf{Z}$ is positive definite (negative definite), and $\lambda_{\min}(\mathbf{Z})$ and $\lambda_{\max}(\mathbf{Z})$ represent the

minimum and maximum eigenvalue of matrix $\mathbf{Z}$. In addition, $\|\mathbf{y}\|_1$, $\|\mathbf{y}\|_2$ and $\|\mathbf{y}\|_\infty$ represent the L1-norm, L2-norm and Linfinite-norm of $\mathbf{y}$ respectively.

First, the typical nonlinear dynamic model to represent the master or local device is used, that is,

$$\mathbf{M_m}(\mathbf{q_m})\ddot{\mathbf{q}}_\mathbf{m} + \mathbf{C_m}(\mathbf{q_m}, \dot{\mathbf{q}}_\mathbf{m})\dot{\mathbf{q}}_\mathbf{m} + \mathbf{g_m}(\mathbf{q_m}) = \boldsymbol{\tau}_\mathbf{m} + \mathbf{f_h} \tag{1}$$

Where $\mathbf{q_m}(t) \in R^{n\times 1}$ is the joint position of the master; $\dot{\mathbf{q}}_\mathbf{m}(t)$ is the joint velocity; $\mathbf{M_m}(\mathbf{q_m}) \in R^{n\times n}$ is the inertia matrix; $\mathbf{C_m}(\mathbf{q_m}, \dot{\mathbf{q}}_\mathbf{m})$ is the matrix representing centripetal and coriolis torques; $\mathbf{g_m}(\mathbf{q_m})$ is the gravitational torque; $\mathbf{f_h}$ is the torque caused by the human operator force and $\boldsymbol{\tau}_\mathbf{m}$ is the control torque applied to the master.

For the case of teleoperation of a wheeled robot, the dynamic model of a unicycle-type mobile robot is considered [15]. It has two independently actuated rear wheels and is represented by,

$$\mathbf{D}\dot{\boldsymbol{\eta}} + \mathbf{Q}(\boldsymbol{\eta})\boldsymbol{\eta} = \boldsymbol{\tau}_\mathbf{s} + \mathbf{f_e} \tag{2}$$

Where $\boldsymbol{\eta} = \begin{bmatrix} v \\ \omega \end{bmatrix}$ is the robot velocity vector with v and ω representing the linear and angular velocity of the mobile robot, $\mathbf{f_e}$ is the force caused by the elements of the environment on the robot as well as other non-modeled external forces such as static and dynamic frictions, $\mathbf{D} = \begin{bmatrix} m & 0 \\ 0 & i \end{bmatrix}$ is the inertia matrix and $\mathbf{Q} = \begin{bmatrix} 0 & -ma\omega \\ ma\omega & 0 \end{bmatrix}$ is the coriolis matrix where m is the mass of the robot, i is the rotational inertia, and a is the distance between the mass center and the geometric center. In addition, $\boldsymbol{\tau}_\mathbf{s} = \begin{bmatrix} u_1 \\ u_2 \end{bmatrix}$ involves a control force u_1 and a control torque u_2, with $u_1 = \frac{1}{r_w}(u_{left} + u_{right})$ and $u_2 = \frac{c}{r_w}(u_{right} - u_{left})$ where $r_w > 0$ is the radius of the wheels, $c > 0$ is the half-width of the cart, and u_{left} and u_{right} are the torques of the left and right rear wheels respectively. Furthermore, the communication channel adds a forward time delay h_1 (from the master to the slave) and a backward time delay h_2 (from the slave to the master). Generally, these delays are time-varying and different between them (asymmetric delays).

On the other hand, the following ordinary properties, assumptions and lemmas will be used in this paper [6],[18]:

Property 1: The inertia matrices $\mathbf{M_m}(\mathbf{q_m})$ and $\mathbf{D}$ are symmetric positive definite. The matrix $\mathbf{D}$ is assumed constant.

Property 2: The matrix $\dot{\mathbf{M}}_\mathbf{m}(\mathbf{q_m}) - 2\mathbf{C_m}(\mathbf{q_m}, \dot{\mathbf{q}}_\mathbf{m})$ is skew-symmetric.

Property 3: There exists a $k_r > 0$ such that $\mathbf{C_m}(\mathbf{q_m}, \dot{\mathbf{q}}_\mathbf{m})\dot{\mathbf{q}}_\mathbf{m} \le k_r|\dot{\mathbf{q}}_\mathbf{m}|$ for all time t.

Assumption 1: The time delays $h_1(t)$ and $h_2(t)$ are bounded. Therefore, there exist positive scalars $\bar{h}_1$ and $\bar{h}_2$ such that $0 \le h_1(t) \le \bar{h}_1$ and $0 \le h_2(t) \le \bar{h}_2$ for all t.

Assumption 2: The human operator and the environment behave in a non-passive way and they are represented by the following models,

$$\mathbf{f_h} = -\alpha_h \dot{\mathbf{q}}_\mathbf{m} + \mathbf{f}_{a_h} \tag{3}$$

$$\mathbf{f_e} = -\alpha_e \boldsymbol{\eta} + \mathbf{f}_{a_e} \tag{4}$$

where α_h is the damping of the human operator model, and α_e is the environment's damping (passive components). On the other hand, $\mathbf{f}_{a_h}$ and $\mathbf{f}_{a_e}$ involve non-passive and additional passive components which are assumed bounded, that is $|\mathbf{f}_{\mathbf{a}_h}| \le \bar{f}_{a_h}$ and $|\mathbf{f}_{\mathbf{a_e}}| \le \bar{f}_{a_e}$, with $\bar{f}_{a_h}$ and $\bar{f}_{a_e}$ positive constants.

Assumption 3: The jerk of the mobile robot $\dddot{\boldsymbol{\eta}}$ is considered bounded, that is $|\dddot{\boldsymbol{\eta}}| \le \beta$, where β is a positive constant.

Lemma 1 [18]**:** For real vector functions $\mathbf{a}(.)$ and $\mathbf{b}(.)$ and a time-varying scalar $h(t)$ with $0 \le h(t) \le \bar{h}$, the following inequality holds,

$$\begin{aligned} &-2\mathbf{a}^T(t)\int_{t-h(t)}^{t}\mathbf{b}(\xi)d\xi - \int_{t-h(t)}^{t}\mathbf{b}^T(\xi)\mathbf{b}(\xi)d\xi \\ &\le h(t)\mathbf{a}^T(t)\mathbf{a}(t) \le \bar{h}(t)\mathbf{a}^T(t)\mathbf{a}(t) \end{aligned} \tag{5}$$

In the next section, the control scheme will be introduced.

III. PD-LIKE CONTROLLER FOR TELEOPERATION

It is known that PD-like controllers are simple structures that generally have a good performance in practice for common applications and are calibrated quickly. Lately, the performance of these schemes was evaluated for the position control in bilateral teleoperation systems of manipulator robots [6], [18]. In these cases, if the damping of the master and slave are sufficiently big, then the stability is assured. If the damping increases, the system is better in terms of stability but the transparency is worst [18].

Here, the teleoperation system is used to control the velocity of a mobile robot, where the user permanently sends commands and perceives by means of force feedback the remote task. The human-centered PD-like controller proposed, establish the control actions as follows,

$$\begin{cases} \boldsymbol{\tau}_\mathbf{m} = -k_m\left(k_g\mathbf{q}_\mathbf{m}(t) - \boldsymbol{\eta}(t-h_2)\right) - \alpha_m\dot{\mathbf{q}}_\mathbf{m} - k_p\mathbf{q}_\mathbf{m} + \mathbf{g}_\mathbf{m}(\mathbf{q}_\mathbf{m}) \\ \boldsymbol{\tau}_\mathbf{s} = k_s\left(k_g\mathbf{q}_\mathbf{m}(t-h_1) - \boldsymbol{\eta}\right) - \sigma_s\mathbf{z} + \mathbf{Q}(\boldsymbol{\eta})\boldsymbol{\eta} \end{cases} \tag{6}$$

Where the controller is formed by $\boldsymbol{\tau}_\mathbf{m}$ and $\boldsymbol{\tau}_\mathbf{s}$. The parameters k_s and α_s are positive constant and they represent the proportional gain and acceleration dependent damping added by the velocity controller, α_m, k_p are the damping and spring injected in the master, and k_m represents

a relative spring depending on the mismatch between the master reference and the mobile robot velocity.

Besides, the parameter k_g linearly maps the master position to a velocity reference, and $\mathbf{z}$ represents the mobile robot acceleration $\dot{\boldsymbol{\eta}}$ at an infinitesimal time instant before t, that is

$$\dot{\boldsymbol{\eta}} = \mathbf{z} + \gamma \dot{\mathbf{z}} \tag{7}$$

with $\gamma \to 0^+$. Next, the stability of the delayed bilateral teleoperation system modeled by (1), (2), (3), (4), the communication channel and the PD-like controller (5) will be analyzed.

Remark 1: In practice most controllers are implemented in discrete-time. In this case $\mathbf{z}$ represents the mobile robot acceleration $\dot{\boldsymbol{\eta}}$ obtained in last sampling time k-1 previous to the current sample k.

Remark 2: It is important to signal that the whole system is nonlinear and includes asymmetric time-varying delays. The compensation terms used in (6) only allow linearizing the mobile robot dynamics but not the master dynamics.

Remark 3: The control scheme does not compensate the non-modeled external forces but they are felt by the human operator since such forces, represented by the term $\mathbf{f}_{a_e}$ in (4), change the mobile robot motion and therefore the force feedback received by the user.

IV. STABILITY OF THE DELAYED CLOSED-LOOP SYSTEM

The stability analysis of the control scheme is based on a Lyapunov-Krasovskii functional (LKF) [25] applied to bilateral teleoperation of a mobile robot. Now, we present the main result of this work as follows.

Theorem 1: Consider a delayed teleoperation system, where a human operator (3) using a master device (1), drives a remote mobile robot described by (2) and (7) interacting with an environment (4), and where the control law (6) is included. For positive constant parameters k_m, k_s, k_g considering Assumptions **1**, **2** and **3** and Properties **1**, **2** and **3**; if the control parameters α_m and σ_s are such that the following inequalities hold:

$$-\lambda_m = -\alpha_m + k_g{}^2 \bar{h}_1 + \frac{1}{4}\bar{h}_2 k_m{}^2 < 0$$

$$-\lambda_s = \frac{k_m}{k_s k_g}\left(-\sigma_s - |\mathbf{D}|\right) + \frac{1}{4}\bar{h}_1 \frac{k_m{}^2}{k_g{}^2} + \bar{h}_2 < 0$$

then the vector $\mathbf{x} = \begin{bmatrix} \mathbf{q_m} & \dot{\mathbf{q}}_\mathbf{m} & k_g \mathbf{q_m} - \boldsymbol{\eta} & \mathbf{z} & \boldsymbol{\eta} \end{bmatrix} \in L_\infty$. In addition, the variables $\dot{\mathbf{q}}_\mathbf{m}$ and $\mathbf{z}$ are ultimately bounded to a convergence zone given by $\max\left(\frac{\rho_m}{\lambda_m}, \frac{\rho_s}{\lambda_s}\right)$, where $\rho_m = \bar{f}_{a_h}$ and $\rho_s = \frac{k_m}{k_s k_g}\bar{f}_{a_e}$.

Proof: First, a functional $V = V_1 + V_2 + V_3 + V_4 + V_5 + V_6 > 0$ is proposed in order to analyze its evolution along the system trajectories. It is formed by six parts: V_1 represents the kinetic energy of the master, V_2 considers the potential energy of the error between the master and the mobile robot, V_3, V_4 taking into account the motion energy of the mobile robot, V_5 represents the potential energy of the master, and V_6 is included for mathematical reasons in order to transform the terms that include delayed variables to terms with non-delayed variables. The first five sub-functional are defined in the following manner:

$$V_1 = \frac{1}{2}\dot{\mathbf{q}}_\mathbf{m}^{\mathrm{T}}\mathbf{M}_\mathbf{m}(\mathbf{q}_\mathbf{m})\dot{\mathbf{q}}_\mathbf{m} \tag{8}$$

$$V_2 = \frac{1}{2}\frac{k_m}{k_g}\left(k_g\mathbf{q}_\mathbf{m} - \boldsymbol{\eta}\right)^{\mathrm{T}}\left(k_g\mathbf{q}_\mathbf{m} - \boldsymbol{\eta}\right) \tag{9}$$

$$V_3 = \frac{1}{2}\alpha_e\frac{k_m}{k_s k_g}\boldsymbol{\eta}^{\mathrm{T}}\boldsymbol{\eta} \tag{10}$$

$$V_4 = \frac{1}{2}\gamma\frac{k_m}{k_s k_g}\mathbf{z}^{\mathrm{T}}\mathbf{D}\mathbf{z} \tag{11}$$

$$V_5 = \frac{1}{2}k_p\mathbf{q}_\mathbf{m}^{\mathrm{T}}\mathbf{q}_\mathbf{m} \tag{12}$$

The time derivative of V_1 (8) along the master dynamics (1), taking into account properties **1** and **2**, is the following one,

$$\begin{aligned}\dot{V}_1 &= \frac{1}{2}\dot{\mathbf{q}}_\mathbf{m}^{\mathrm{T}}\dot{\mathbf{M}}_\mathbf{m}\dot{\mathbf{q}}_\mathbf{m} + \dot{\mathbf{q}}_\mathbf{m}^{\mathrm{T}}\mathbf{M}_\mathbf{m}\ddot{\mathbf{q}}_\mathbf{m} \\ &= \frac{1}{2}\dot{\mathbf{q}}_\mathbf{m}^{\mathrm{T}}\dot{\mathbf{M}}_\mathbf{m}\dot{\mathbf{q}}_\mathbf{m} + \\ &\quad \dot{\mathbf{q}}_\mathbf{m}^{\mathrm{T}}\mathbf{M}_\mathbf{m}\mathbf{M}_\mathbf{m}^{-1}\left(\boldsymbol{\tau}_\mathbf{m} + \mathbf{f}_\mathbf{h} - \mathbf{g}(\mathbf{q}_\mathbf{m}) - \mathbf{C}_\mathbf{m}\dot{\mathbf{q}}_\mathbf{m}\right) \\ &= \dot{\mathbf{q}}_\mathbf{m}^{\mathrm{T}}\left(\boldsymbol{\tau}_\mathbf{m} + \mathbf{f}_\mathbf{h} - \mathbf{g}(\mathbf{q}_\mathbf{m})\right)\end{aligned} \tag{13}$$

Now, if the control action $\boldsymbol{\tau}_\mathbf{m}$ of (6) is included in (13) considering also (3), it yields,

$$\begin{aligned}\dot{V}_1 &= \dot{\mathbf{q}}_\mathbf{m}^{\mathrm{T}}\left(\boldsymbol{\tau}_\mathbf{m} - \mathbf{g}_\mathbf{m}(\mathbf{q}_\mathbf{m})\right) + \dot{\mathbf{q}}_\mathbf{m}^{\mathrm{T}}\mathbf{f}_\mathbf{h} \\ &= \dot{\mathbf{q}}_\mathbf{m}^{\mathrm{T}}\left(-k_m\left(k_g\mathbf{q}_\mathbf{m} - \boldsymbol{\eta}(t-h_2)\right) - \alpha_m\dot{\mathbf{q}}_\mathbf{m}\right) \\ &\quad + \dot{\mathbf{q}}_\mathbf{m}^{\mathrm{T}}\left(\mathbf{f}_{\mathbf{a}_\mathbf{h}} - \alpha_h\dot{\mathbf{q}}_\mathbf{m} - k_p\mathbf{q}_\mathbf{m}\right) \\ &= -k_m\dot{\mathbf{q}}_\mathbf{m}^{\mathrm{T}}\left(\left(k_g\mathbf{q}_\mathbf{m} - \boldsymbol{\eta}(t-h_2) + \boldsymbol{\eta} - \boldsymbol{\eta}\right)\right) - \left(\alpha_m + \alpha_h\right)\dot{\mathbf{q}}_\mathbf{m}^{\mathrm{T}}\dot{\mathbf{q}}_\mathbf{m} \\ &\quad - k_h\dot{\mathbf{q}}_\mathbf{m}^{\mathrm{T}}\mathbf{q}_\mathbf{m} + \dot{\mathbf{q}}_\mathbf{m}^{\mathrm{T}}\mathbf{f}_{\mathbf{a}_\mathbf{h}} \\ &= -\left(\alpha_m + \alpha_h\right)\dot{\mathbf{q}}_\mathbf{m}^{\mathrm{T}}\dot{\mathbf{q}}_\mathbf{m} - k_m\dot{\mathbf{q}}_\mathbf{m}^{\mathrm{T}}\left(k_g\mathbf{q}_\mathbf{m} - \boldsymbol{\eta}\right) \\ &\quad - k_m\dot{\mathbf{q}}_\mathbf{m}^{\mathrm{T}}\int_{t-h_2}^{t}\dot{\boldsymbol{\eta}}(\xi)d\xi - k_p\dot{\mathbf{q}}_\mathbf{m}^{\mathrm{T}}\mathbf{q}_\mathbf{m} + \dot{\mathbf{q}}_\mathbf{m}^{\mathrm{T}}\mathbf{f}_{\mathbf{a}_\mathbf{h}}\end{aligned} \tag{14}$$

Next, $\dot{V}_2$ is obtained from (9) considering (7) as well as assumption **3**, as follows,

$$\begin{aligned}\dot{\mathrm{V}}_2 &= \frac{k_m}{k_g}\left(k_g\mathbf{q_m}-\boldsymbol{\eta}\right)^{\mathrm{T}}\left(k_g\dot{\mathbf{q}}_{\mathbf{m}}-\dot{\boldsymbol{\eta}}\right)\\ &\approx -\frac{k_m}{k_g}\left(k_g\mathbf{q_m}-\boldsymbol{\eta}\right)^{\mathrm{T}}\mathbf{z}+k_m\left(k_g\mathbf{q_m}-\boldsymbol{\eta}\right)^{\mathrm{T}}\dot{\mathbf{q}}_{\mathbf{m}}\end{aligned} \tag{15}$$

On the other hand, $\dot{\mathrm{V}}_3$ is computed from (10) taking into account (7) and assumption **3**, as follows,

$$\dot{\mathrm{V}}_3 = \alpha_e\frac{k_m}{k_sk_g}\boldsymbol{\eta}^{\mathrm{T}}\dot{\boldsymbol{\eta}} \approx \alpha_e\frac{k_m}{k_sk_g}\boldsymbol{\eta}^{\mathrm{T}}\mathbf{z} \tag{16}$$

Besides, $\dot{\mathrm{V}}_4$ along the mobile robot dynamics (2) can be written including (6) into the derivative of (11), in the following way,

$$\begin{aligned}\dot{\mathrm{V}}_4 &= \gamma\frac{k_m}{k_sk_g}\mathbf{z}^{\mathrm{T}}\mathbf{D}\dot{\mathbf{z}} = \gamma\frac{k_m}{k_sk_g}\mathbf{z}^{\mathrm{T}}\mathbf{D}\left(\frac{\dot{\boldsymbol{\eta}}}{\gamma}-\frac{\mathbf{z}}{\gamma}\right)\\ &= \frac{k_m}{k_sk_g}\mathbf{z}^{\mathrm{T}}\mathbf{D}\dot{\boldsymbol{\eta}}-\frac{k_m}{k_sk_g}\mathbf{z}^{\mathrm{T}}\mathbf{D}\mathbf{z}\\ &= -\sigma_s\frac{k_m}{k_sk_g}\mathbf{z}^{\mathrm{T}}\mathbf{z}+\frac{k_m}{k_sk_g}\mathbf{z}^{\mathrm{T}}\mathbf{f_e}-\frac{k_m}{k_sk_g}\mathbf{z}^{\mathrm{T}}\mathbf{D}\mathbf{z}\\ &\quad+\frac{k_m}{k_g}\mathbf{z}^{\mathrm{T}}\left(k_g\mathbf{q_m}(t-h_1)+k_g\mathbf{q_m}-k_g\mathbf{q_m}-\boldsymbol{\eta}\right)\\ &= -\sigma_s\frac{k_m}{k_sk_g}\mathbf{z}^{\mathrm{T}}\mathbf{z}+\frac{k_m}{k_g}\mathbf{z}^{\mathrm{T}}\left(k_g\mathbf{q_m}-\boldsymbol{\eta}\right)-\alpha_e\frac{k_m}{k_sk_g}\mathbf{z}^{\mathrm{T}}\boldsymbol{\eta}\\ &\quad+\frac{k_m}{k_sk_g}\mathbf{z}^{\mathrm{T}}\mathbf{f_{a_e}}-\frac{k_m}{k_sk_g}\mathbf{z}^{\mathrm{T}}\mathbf{D}\mathbf{z}-k_m\mathbf{z}^{\mathrm{T}}\int_{t-h_1}^{t}\dot{\mathbf{q}}_{\mathbf{m}}(\xi)d\xi\end{aligned} \tag{17}$$

Furthermore, $\dot{\mathrm{V}}_5$ is obtained from (12) as follows,

$$\dot{\mathrm{V}}_5 = k_p\mathbf{q_m}^{\mathrm{T}}\dot{\mathbf{q}}_{\mathbf{m}} \tag{18}$$

It is possible to appreciate in (14) and (17) that there are terms with delayed variables that make the stability analysis difficult. For solving this, V_6 is proposed as follows:

$$\begin{aligned}\mathrm{V}_6 &= \int_{-\bar{h}_2}^{0}\int_{t+\theta}^{t}\mathbf{z}(\xi)^{\mathrm{T}}\mathbf{z}(\xi)d\xi d\theta\\ &\quad+k_g{}^2\int_{-\bar{h}_1}^{0}\int_{t+\theta}^{t}\dot{\mathbf{q}}_{\mathbf{m}}(\xi)^{\mathrm{T}}\dot{\mathbf{q}}_{\mathbf{m}}(\xi)d\xi d\theta\end{aligned} \tag{19}$$

From (19), and considering assumption **1**, $\dot{\mathrm{V}}_6$ is computed by,

$$\begin{aligned}\dot{\mathrm{V}}_6 &\le \bar{h}_2\mathbf{z}^{\mathrm{T}}\mathbf{z}-\int_{t-h_2}^{t}\mathbf{z}^{\mathrm{T}}(\xi)\mathbf{z}(\xi)d\xi\\ &\quad+k_g{}^2\bar{h}_1\dot{\mathbf{q}}_{\mathbf{m}}{}^{\mathrm{T}}\dot{\mathbf{q}}_{\mathbf{m}}-k_g{}^2\int_{t-h_1}^{t}\dot{\mathbf{q}}_{\mathbf{m}}{}^{\mathrm{T}}(\xi)\dot{\mathbf{q}}_{\mathbf{m}}(\xi)d\xi\end{aligned} \tag{20}$$

The terms with integrals of (20) can be linked with the third term of (14) and the sixth term of (17) by using Lemma **1** (5), which considering (7) yields,

$$
\begin{aligned}
&-k_m \mathbf{z}^{\mathbf{T}} \int_{t-h_1}^{t} \dot{\mathbf{q}}_{\mathbf{m}}(\xi)\, d\xi - {k_g}^2 \int_{t-h_1}^{t} \dot{\mathbf{q}}_{\mathbf{m}}{}^{\mathbf{T}}(\xi)\, \dot{\mathbf{q}}_{\mathbf{m}}(\xi)\, d\xi \\
&\leq \frac{1}{4} \bar{h}_1 \frac{{k_m}^2}{{k_g}^2} \mathbf{z}^{\mathbf{T}} \mathbf{z}
\end{aligned} \tag{21}
$$

$$
\begin{aligned}
&- \int_{t-h_2}^{t} \mathbf{z}^{\mathbf{T}}(\xi) \mathbf{z}(\xi) d\xi - k_m \dot{\mathbf{q}}_{\mathbf{m}}{}^{\mathbf{T}} \int_{t-h_2}^{t} \dot{\boldsymbol{\eta}}(\xi) d\xi \\
&= - \int_{t-h_2}^{t} \mathbf{z}^{\mathbf{T}}(\xi) \mathbf{z}(\xi) d\xi - k_m \dot{\mathbf{q}}_{\mathbf{m}}{}^{\mathbf{T}} \int_{t-h_2}^{t} \left(\mathbf{z}(\xi) + \gamma\, \dot{\mathbf{z}}(\xi) \right) d\xi \\
&\leq \frac{1}{4} \bar{h}_2 {k_m}^2 \dot{\mathbf{q}}_{\mathbf{m}}{}^{\mathbf{T}} \dot{\mathbf{q}}_{\mathbf{m}} + k_m \gamma \beta \bar{h}_2 |\dot{\mathbf{q}}_{\mathbf{m}}| \\
&\approx \frac{1}{4} \bar{h}_2 {k_m}^2 \dot{\mathbf{q}}_{\mathbf{m}}{}^{\mathbf{T}} \dot{\mathbf{q}}_{\mathbf{m}}
\end{aligned} \tag{22}
$$

That is, the terms with integrals were replaced by common quadratic terms. Finally, $\dot{\mathrm{V}}$ can be built joining (14), (15), (16), (17), (18) and (20) considering the relations (21) and (22) as follows,

$$
\begin{aligned}
\dot{\mathrm{V}} &= \dot{\mathrm{V}}_1 + \dot{\mathrm{V}}_2 + \dot{\mathrm{V}}_3 + \dot{\mathrm{V}}_4 + \dot{\mathrm{V}}_5 \\
&\leq \dot{\mathbf{q}}_{\mathbf{m}}{}^{\mathbf{T}} \left[-\alpha_m \mathbf{I} + {k_g}^2 \bar{h}_1 \mathbf{I} + \frac{1}{4} \bar{h}_2 {k_m}^2 \mathbf{I} \right] \dot{\mathbf{q}}_{\mathbf{m}} \\
&+ \mathbf{z}^{\mathbf{T}} \left[\frac{k_m}{k_s k_g} \left(-\sigma_s \mathbf{I} - \mathbf{D} \right) + \frac{1}{4} \bar{h}_1 \frac{{k_m}^2}{{k_g}^2} \mathbf{I} + \bar{h}_2 \mathbf{I} \right] \mathbf{z} \\
&+ \frac{k_m}{k_s k_g} \bar{f}_{a_e} |\mathbf{z}| + \bar{f}_{a_h} |\dot{\mathbf{q}}_{\mathbf{m}}| \\
&= -\lambda_m \dot{\mathbf{q}}_{\mathbf{m}}{}^{\mathbf{T}} \dot{\mathbf{q}}_{\mathbf{m}} - \lambda_s \mathbf{z}^{\mathbf{T}} \mathbf{z} + \rho_m |\dot{\mathbf{q}}_{\mathbf{m}}| + \rho_s |\mathbf{z}|
\end{aligned} \tag{23}
$$

Given a positive constant parameters for k_m, k_s, and k_g as well as bounded values for $\bar{h}_1$, $\bar{h}_2$, $\bar{f}_{a_e}$ and $\bar{f}_{a_h}$, the control parameters α_m and σ_s can be set to guarantee that the first two terms of (23) are negative definite and therefore the variables $\mathbf{q}_{\mathbf{m}}, \dot{\mathbf{q}}_{\mathbf{m}}, k_g \mathbf{q}_{\mathbf{m}} - \boldsymbol{\eta}, \mathbf{z}, \boldsymbol{\eta} \in L_\infty$. For this condition, it is possible to appreciate from (23) that the state variables $\dot{\mathbf{q}}_{\mathbf{m}}$ and $\mathbf{z}$ are ultimately bounded to a convergence zone established by the $\max\left(\frac{\rho_m}{\lambda_m}, \frac{\rho_s}{\lambda_s} \right)$. The proof is completed.

Remark 4: If the components of the human operator $\mathbf{f}_{\mathbf{a_h}}$ and environment $\mathbf{f}_{\mathbf{a_e}}$ are null ($\bar{f}_{a_h} = \bar{f}_{a_e} = 0$), then $\rho_m = \rho_s = 0$ and therefore the system is stable. For this particular case, the Barbalat's lemma can be used in (23), where taking into account assumptions **1**, **2** and **3**, property **3** and that $\mathbf{q}_{\mathbf{m}}, \dot{\mathbf{q}}_{\mathbf{m}}, k_g \mathbf{q}_{\mathbf{m}} - \boldsymbol{\eta}, \mathbf{z}, \boldsymbol{\eta} \in L_\infty$, it is possible to deduce that $\ddot{\mathbf{q}}_{\mathbf{m}}$ and $\dot{\mathbf{z}}$ are bounded and therefore $\ddot{\mathrm{V}}$ is bounded too. Then $\dot{\mathbf{q}}_{\mathbf{m}}$ and $\mathbf{z}$ will tend to zero as $t \to \infty$.

Remark 5: The stability analysis is mathematically different to the one used on bilateral teleoperation of manipulators robots [18], due to the mismatch between master (manipulator robot) and the slave (mobile robot) and therefore, the result achieved, useful to calibrate the parameters of the controller in bilateral teleoperation of mobile robots, is dissimilar too.

V. HUMAN-IN-THE-LOOP SIMULATIONS

In this section, the proposed control scheme is tested. A human operator drives a 3D simulator of a mobile Robot employing a 3DOF hand-controller with force feedback (only 2 degrees are used in the experiment, one for angular velocity and the other for linear velocity). The master device is a Novint Falcon http://www.novint.com . The goal of the experiment is to push two objects of different weights from its initial position to a target position (zone marked with red in Fig. 3), and then goes the robot to a goal position (marked in green in Fig. 3). The test 1 involves a type-cube object of 2.5 kg and test 2 includes a similar form object but lighter (1.5 kg). The external forces $\mathbf{f_e}$ are simulated using Bullet Physic engine http://bulletphysics.org, running inside the V-REP environment, http://www.coppeliarobotics.com . This engine-environment includes the simulation of gravity, frictions, materials and contact forces, among others. On the master side, a control app developed under MATLAB www.mathworks.com is used to compute the level of force back-fed to the human operator. An app developed in C++ running at 1 Khz drives the master and links the position and force data through share memory. On the other hand, the velocity controller of the mobile robot is implemented directly on V-REP (remote side) by means of a script. In addition, the simulator interchanges data with the external apps through a Remote API. A diagram of the system behavior is shown in figure 2.

Table 1 shows the parameters of the mobile robot and the objects used in V-REP. The parameters $k_g, k_p, k_m, k_s, \alpha_m, \sigma_s$ in section III were taken as scalar, but in general they can be diagonal matrices called $K_g, K_p, K_m, K_s, \alpha_m, \sigma_s$ respectively. The time delays are simulated using FIFO buffer for comparing the performance under similar delay conditions. It is outside of the scope of this work the modeling of some specific type of time delays such as those present in communications via wifi, internet, etc. In this paper, the time delays are taken in a general way as variables, asymmetric and bounded magnitude. For testing the system, $h_1 = 0.5\,[\mathrm{s}]$ and $h_2 = \left(0.3+0.2\sin\left(2\pi 0.1\mathrm{t}\right)\right)[\mathrm{s}]$ are used.

The procedure recommended to set the control parameters is the following one:

1. Taking $K_m \to 0$ (unilateral case), and $h_1 = h_2 \approx 0\,[\mathrm{s}]$, set K_g to establish the maximum velocity command and K_s considering the dynamics of the mobile robot so that a good performance of the velocity controller in the remote side is achieved.
2. Set K_m to match the desired level of force feedback cue considering the different gains between the master and mobile robot. K_p is chosen near zero to avoid interfering with the force feedback.
3. From the values of K_s , K_g and K_m previously chosen, select $\sigma_s > \sigma_{s_{\min}}$ and $\alpha_m > \alpha_{m_{\min}}$ depending on the maximum time delays $\bar{h}_1$ and $\bar{h}_2$, were $\alpha_{m_{\min}}$ and $\sigma_{s_{\min}}$ are obtained from the first and second term of (23) respectively.

Remark 6: It is important to point out that there is not a theoretical constraint to set the parameters K_m, K_s and K_p but only point 3 must be hold to get stability. Items 1 and 2 describe only guidelines to get a good performance in practice.

The control parameters used in the human-in-the-loop simulations are:

$$K_g = \begin{bmatrix} 10 & 0 \\ 0 & 10 \end{bmatrix}, K_m = \begin{bmatrix} 20 & 0 \\ 0 & 15 \end{bmatrix}, K_s = \begin{bmatrix} 40 & 0 \\ 0 & 10 \end{bmatrix},$$
$$\alpha_m = \begin{bmatrix} 100 & 0 \\ 0 & 80 \end{bmatrix}, \sigma_s = \begin{bmatrix} 5 & 0 \\ 0 & 5 \end{bmatrix}$$

Fig. 3 displays the general sequence of motions carried out by the mobile robot. Fig. 4 shows the trajectory followed by the robot and the motion of the objects pushed by the robot for test 1 (object 1) and test 2 (object 2).

Figures 5-8, show the velocity of the mobile robot compared with the reference generated by the operator, as well as the haptic feedback to the user and torque exerted by the robot. In the tests, the mobile robot velocity follows the velocity command of the user between t_0 and t_1 , at time t_1 the robot hits the object and the user can feel this interaction force (fig. 6). The operator constantly corrects the robot path while pushing the type-cube object; these corrections generally are bigger for lighter objects. At t_2 the object was pushed by the robot until the target position so it moves backward from time t_2 to t_3. Then the robot is guided to the goal area (time interval between t_3 and t_4), and finally the user slow down the robot in order to achieve the goal at time t_5 (Fig. 6) while he feels the stopping force too.

It is important to remark that the interaction mainly occurs on the linear velocity and force. That is, figures 7 and 8 show that the angular velocity follows approximately the commands generated by the user, while the corresponding force feedback is low. The disparity between the angular force felt by the operator and exerted by the robot is due to the damping terms are bigger than the synchronization error terms. On the other hand, figure 5 shows that the mobile robot follows the human's commands when there is no interaction with the object. However in the time interval between t_1 and t_2 , the tracking error increases significantly due to the physical contact between the robot and the object. This situation is felt by the human operator through a force feedback. Besides, when the object pushed by the teleoperated robot has a higher mass (test 1), the human operator receives a greater force feedback, which can be in fig. 6. These results will be extended in the next section where a real mobile robot will be teleoperated by different users.

VI. EXPERIMENTAL RESULTS

In this section, experiments are shown in order to test the performance obtained in practice before different human operators driving a Pioneer P3dx mobile robot through a hand controller with force feedback. The master device used is a 3D Novint Falcon . Similar to section V, the task consist on pushing a box from its initial position to a goal position (marked in blue) and them move the remote robot to a finish zone marked in red (Fig.9). A sequence of the

experiment is shown on Fig. 9, and a video about the experiment can be seen in https://youtu.be/9MvBWIJNQD4 . The parameters and delays used are the same employed on section V. To evaluate the performance achieved, two different indexes are used for each operator. The first metrics is called T_{task} , defined as the time to complete the task. Second index called I_e is defined in (24) to measure the coupling or synchronism between master and mobile robot. Table 3 summarizes the results achieved for each human operator using the PD-like control scheme, whose parameters are calibrated from the theoretical analysis.

$$I_e = \begin{bmatrix} I_{ev} \\ I_{e\omega} \end{bmatrix} = \frac{1}{T_{task}} \int_0^{T_{task}} \left| k_g \mathbf{q_m}(t) - \boldsymbol{\eta}(t) \right| dt \tag{24}$$

It is important to point out that all users were able to complete the task successfully. The performance index T_{task} depends on each teleoperator but the controller collaborates to reach a satisfactory performance in spite of the time delay keeping a bounded error I_e, coupling thus the master and the mobile robot in practice.

VII. CONCLUSIONS

In this paper, the stability analysis of a bilateral teleoperation system of a mobile robot has been proposed considering asymmetric and time-varying delays. Such analysis gives as result the correct procedure for calibrating the damping applied into the master and mobile robot, in order to assure the system stability mainly depending on the forward and reverse time delays added by the communication channel. Finally, human-in-the-loop simulations as well as experiments with robots were made, whose results give bounded errors of the main variables of the bilateral teleoperation system of a mobile robot, which is in agreement with the theoretical analysis carried out. In addition, the performance achieved, measured with two typical indexes, is satisfactory for different users.

REFERENCES

[1] R.J. Anderson, and Spong, M., "Bilateral control of Teleoperators with time delay". *IEEE Trans and Automatic Control,* 34(5):494-501 (1989).

[2] P.F. Hokayem and M.W. Spong. "Bilateral: an historical survey". *Automatica* , 42: 2035-2057, (2006).

[3] I. Elhajj, Xi, N., Fung W., Liu Y., *et al*., *Supermedia-Enhanced Internet-Based Telerobotics.* Proceedings of the IEEE, Vol. 91, Nº3, pp. 396-421, March (2003).

[4] G. Niemeyer, and Slotine, J.J.E., "Stable Adaptive Teleoperation", *IEEE Journal of Oceanic Engineering* , 16(1):152-162 (1991).

[5] G. Niemeyer, and Slotine, J., *Telemanipulation with time delays*. Int. Journal of Robotics Research, 23(9): 873-890, (2004).

[6] E. Nuno, R. Ortega, N. Barabanov, and L. Basanez, "A globally stable PD controller for bilateral teleoperators", *IEEE Trans. on Robotics*, vol. 22, no. 3, pp. 753-758, (2008).

[7] J.P. Richard, *Time-delay systems: an overview of some recent advances and open problems*. Automatica 39, pp. 1667-1694 (2003).

[8] T.B. Sheridan, *Telerobotics, Automation, and Human Supervisory Control*. The MIT Press, Cambrige, MA (1992).

[9] T.B. Sheridan, *Space Teleoperation through Time Delay: Review and Prognosis*. IEEE Transactions on Robotics and Automation, Vol. 9, No 5, October (1993).

[10] E. Slawinski, V. Mut and J.F. Postigo, "Teleoperation of mobile robots with time-varying delay", IEEE Trans. on Robotics 23(5):1071-1082, (2007).

[11] I. Farkhatdinov, J-H. Ryu, Jinung An, "A Preliminary Experimental Study on Haptic Teleoperation of Mobile Robot with Variable Force Feedback Gain," In Proc. of IEEE Haptics Symposium 2010, March 24-25, Waltham, Boston, US, (2010).

[12] N. Diolaiti and C. Melchiorri "Haptic teleoperation of a mobile robot," In Proc. of the 7th IFAC SYROCO, pp. 2798-2805, 2003.

[13] S. Lee, G. S. Sukhatme, G. J. Kim, C.-M. Park, "Haptic control of a mobile robot: A user study," In Proc. of IEEE/RSJ IROS 2002, Lausanne, Switzerland, Oct. 2002, pages 2867-2874, (2002).

[14] J. N. Lim, J. P. Ko, and J. M. Lee, "Internet-based Teleoperation of a Mobile Robot with Force-reflection," CCA 2003, Proceedings of 2003 IEEE Conf. on Control Applications, Istanbul, Turkey, June 2003 vol.1 pp.680-685, (2003).

[15] D. Lee, O. Martinez-Palafox, M. W. Spong, "Bilateral teleoperation of a wheeled mobile robot over delayed communication network," In Proc. of IEEE ICRA 2006, pages 3298 – 3303, (2006).

[16] D. Lee and M. Spong, "Passive bilateral teleoperation with constant time delay" IEEE Trans. Robot., vol. 22, no. 2, pp. 269–281, Apr. 2006.

[17] M. Ferre, M. Buss, R. Aracil, C. Melchiorri, and C. Balaguer. *Advances in Telerobotics*. Springer, (2007).

[18] Chang-Chun Hua; Liu, X.P.; "Delay-Dependent Stability Criteria of Teleoperation Systems with Asymmetric Time-Varying Delays," *Robotics, IEEE Trans,* vol.26, no.5, pp.925-932, Oct. 2010.

[19] Xu Z., Ma L, Schilling K. "Passive bilateral teleoperation of a car-like mobile robot". In: Proceedings of 17th mediterranean conference on control & automation; 2009. p. 790–6.

[20] D. A. Lawrence, "Stability and transparency in bilateral teleoperation," IEEE Trans. Robot. Automat., vol. 9, pp. 624–637, Oct. 1993.

[21] E. Slawiñski, V. Mut, L. Salinas and S. García (2012). Teleoperation of a mobile robot with time-varying delay and force feedback. Robotica, 30, pp 67-77.

[22] E. Slawiñski, V. Mut, P. Fiorini and L. Salinas, "Quantitative Absolute Transparency for Bilateral Teleoperation of Mobile Robots," *Systems, Man and Cybernetics, Part A: Systems and Humans, IEEE Transactions on* , vol.42, no.2, pp.430-442, March 2012.

[23] D. Lee; D. Xu; , "Feedback r-passivity of Lagrangian systems for mobile robot teleoperation," *Robotics and Automation (ICRA), 2011 IEEE International Conference on* , vol., no., pp.2118-2123, 9-13 May 2011.

[24] Slawiñski, E. and Mut, V., "PD-like controllers for delayed bilateral teleoperation of manipulators robots", Int. J. Robust Nonlinear Control, Article first published online: 4 April 2014, DOI: 10.1002/rnc.3177.

[25] Emilia Fridman , "Tutorial on Lyapunov-based methods for time-delay systems", European Journal of Control. In press, available online 12 October 2014.

[26] Bo Zhang, Alexandre Kruszewski and Jean-Pierre Richard, "A novel control design for delayed teleoperation based on delay-scheduled Lyapunov-Krasovskii functionals", Int. Journal of Control, Vol. 87, Nº 8, pp. 1694-1706, 2014.

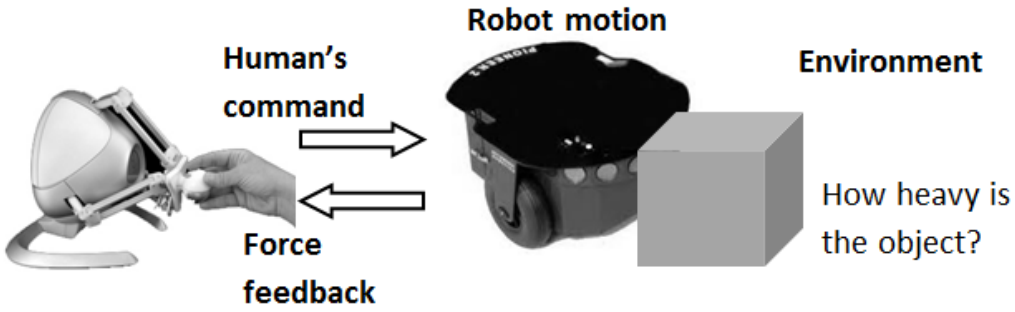

Fig. 1. General delayed teleoperation system.

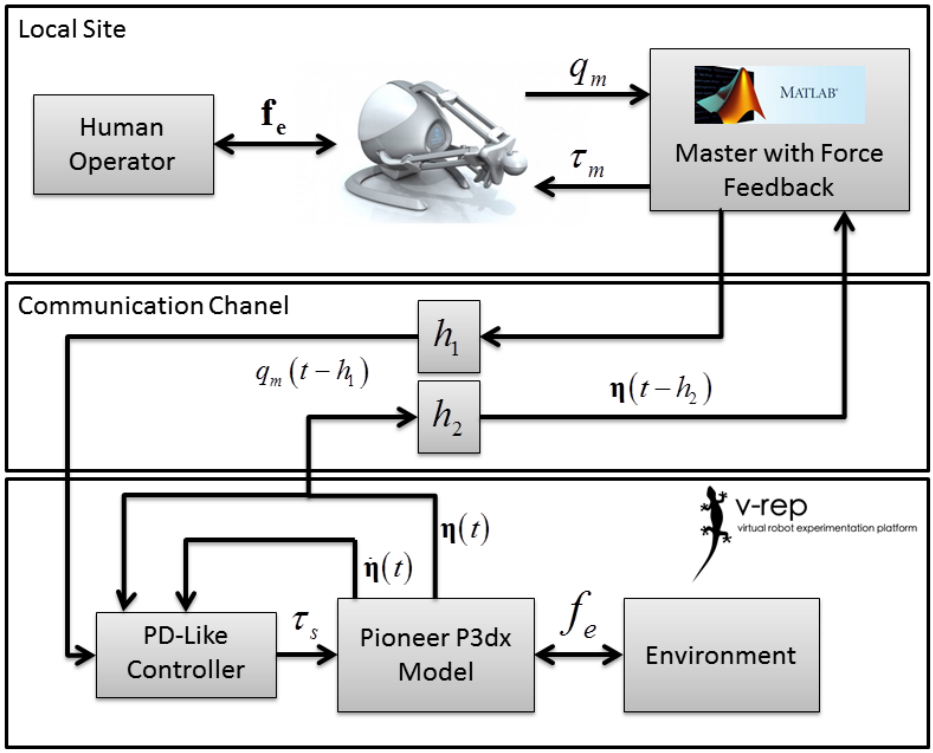

Fig. 2. Block diagram of the teleoperation system.

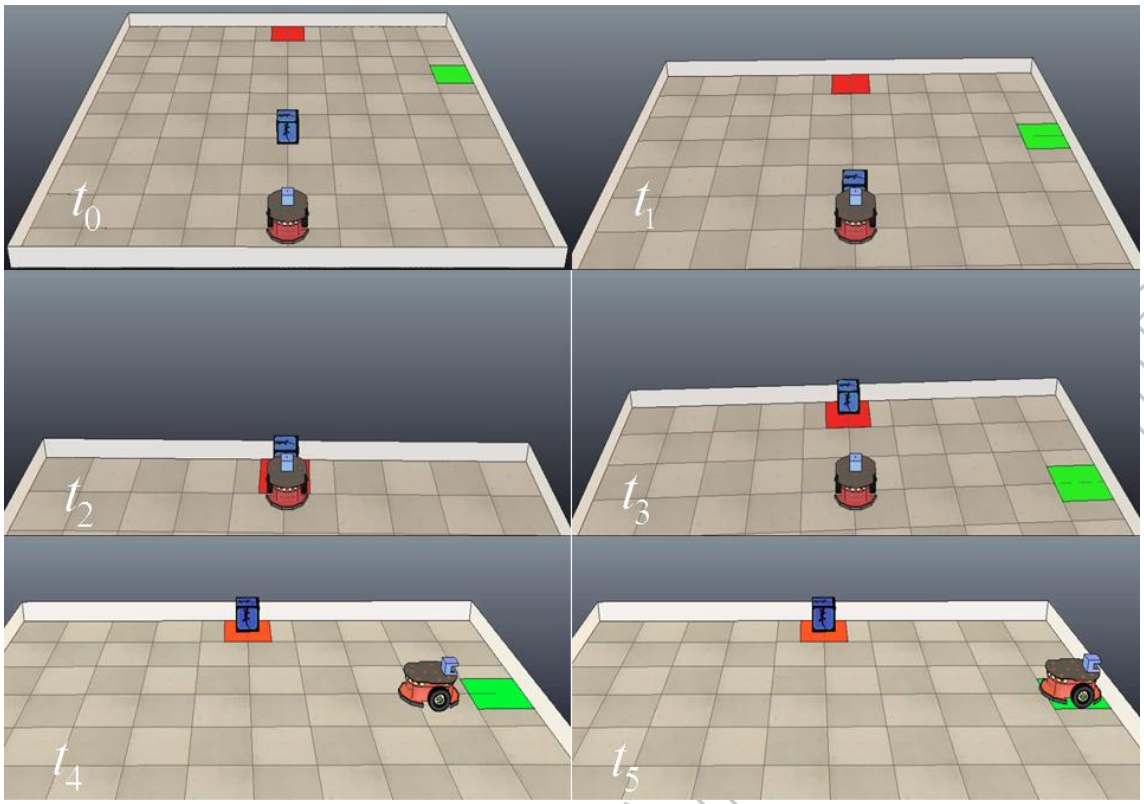

Fig. 3. Time sequence of the mobile robot movement

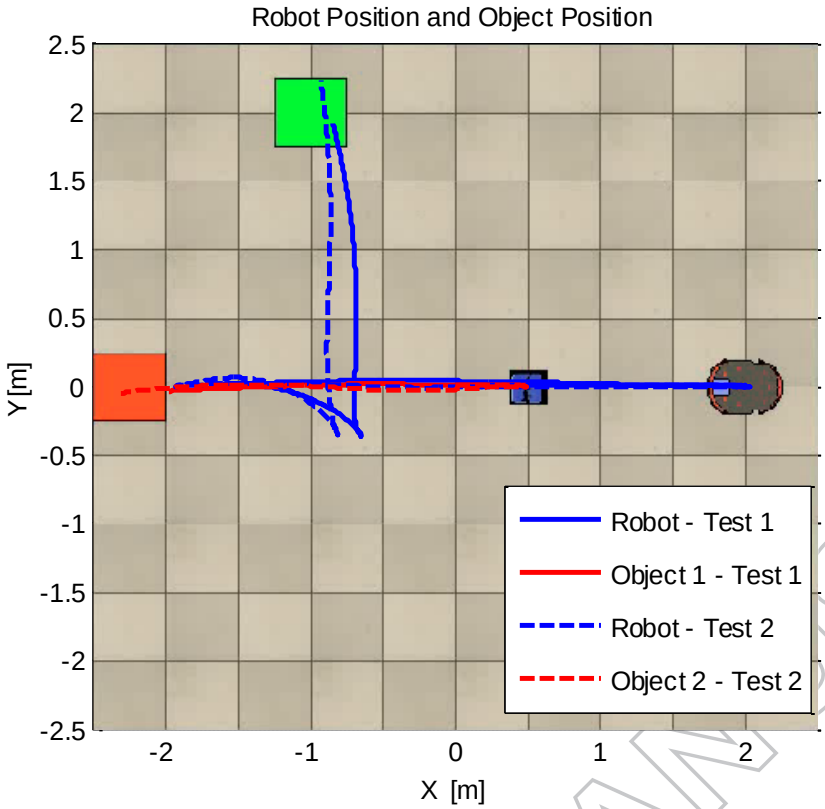

Fig 4. Path followed by the mobile robot (blue) and box (red).

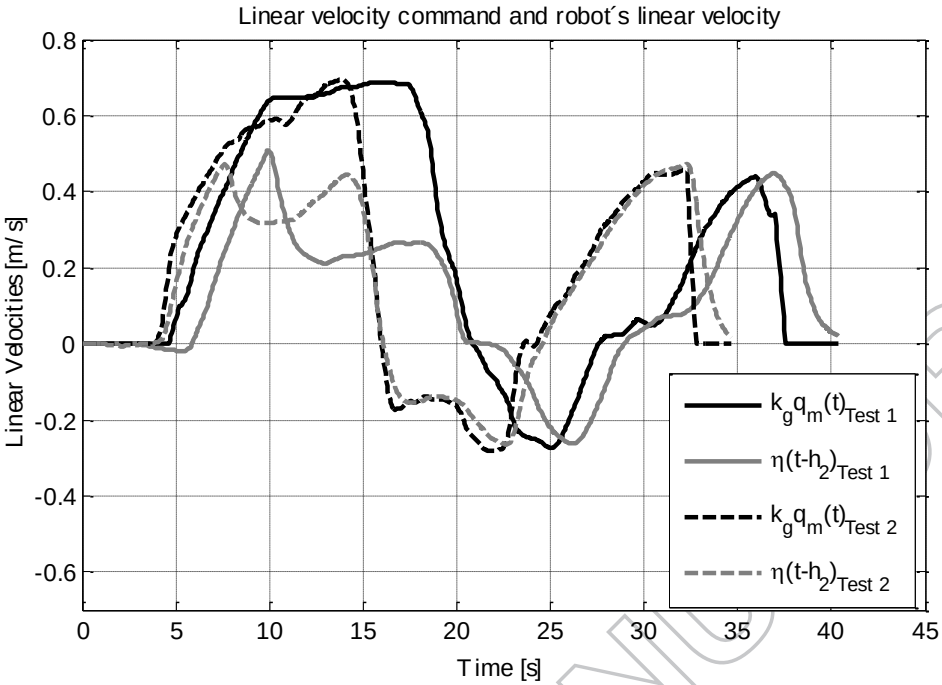

Fig. 5. Mobile robot linear velocity and reference from user.

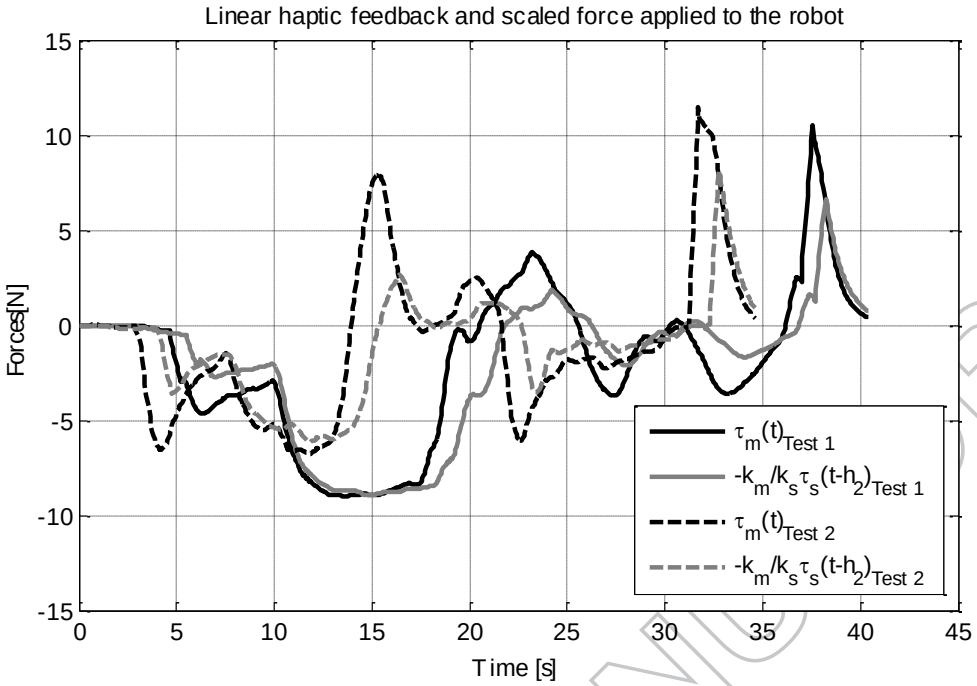

Fig. 6. Linear haptic feedback and scaled force applied to the robot.

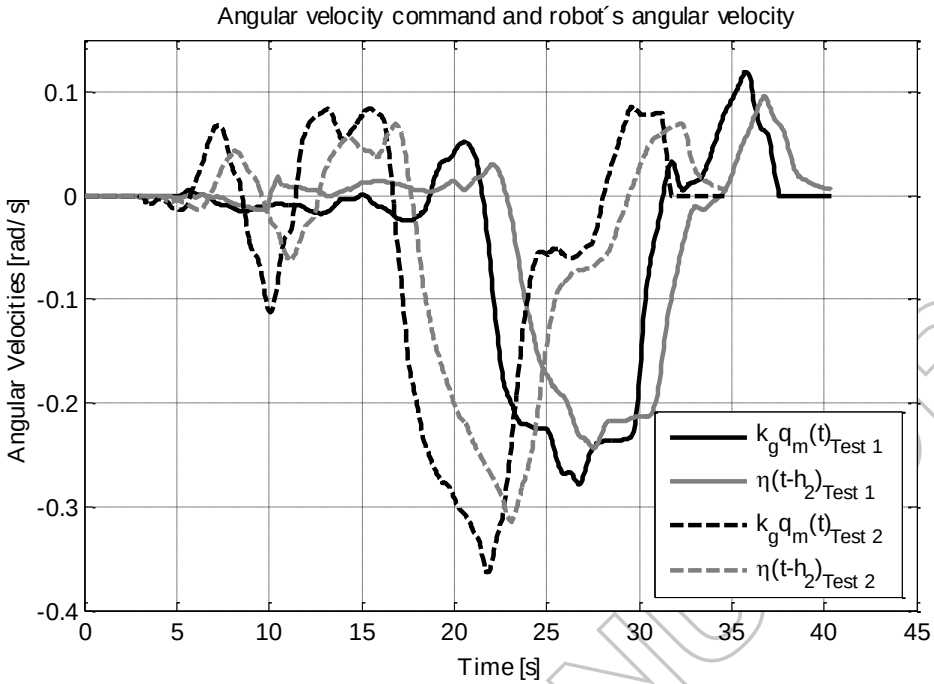

Fig. 7. Mobile robot angular velocity and reference of the master.

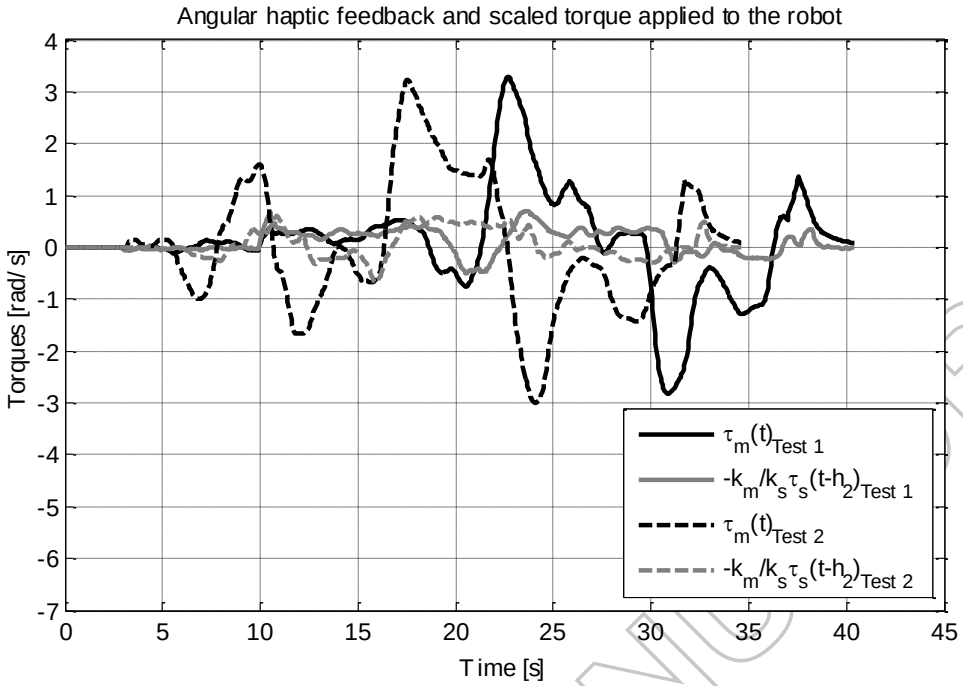

Fig. 8. Haptic torque feedback and scaled torque applied to the robot.

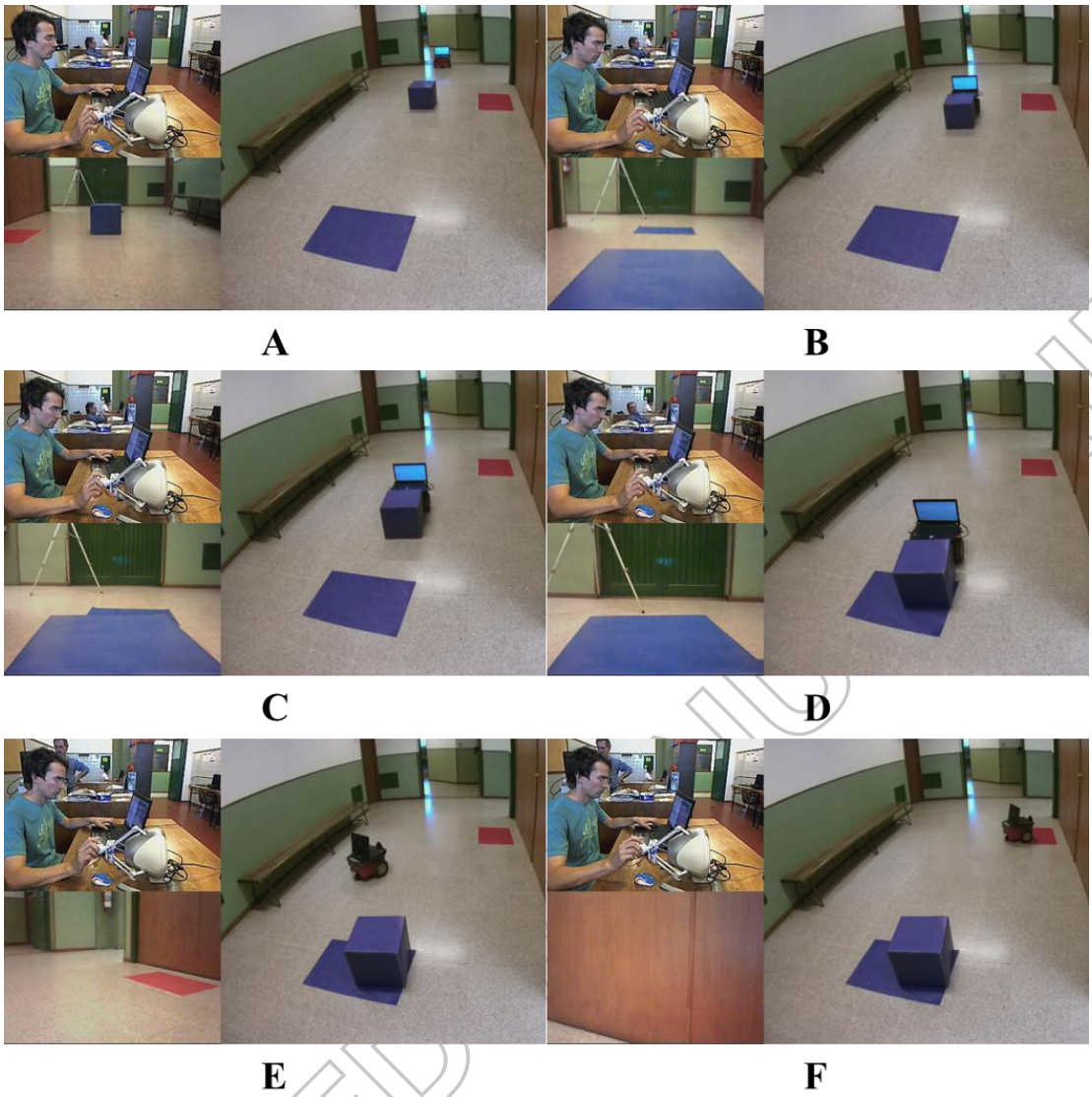

Fig. 9 Experiment sequence

Table 1. Simulation parameters.

Element	Mass $[kg]$	Inertia	Friction
Robot main Body	16.0	$\begin{bmatrix} 0.12 & 0 & 0 \\ 0 & 0.12 & 0 \\ 0 & 0 & 0.13 \end{bmatrix}$	1.0
Left and Right Wheel	1.5	$\begin{bmatrix} 0.02 & 0 & 0 \\ 0 & 0.02 & 0 \\ 0 & 0 & 0.04 \end{bmatrix}$	1.0
Caster link	1.0	$\begin{bmatrix} 0.016 & 0 & 0 \\ 0 & 0.016 & 0 \\ 0 & 0 & 0.02 \end{bmatrix}$	0
Caster wheel	0.25	$\begin{bmatrix} 0.004 & 0 & 0 \\ 0 & 0.004 & 0 \\ 0 & 0 & 0.028 \end{bmatrix}$	0
Object 1	2.5	$\begin{bmatrix} 0.02 & 0 & 0 \\ 0 & 0.02 & 0 \\ 0 & 0 & 0.02 \end{bmatrix}$	0.71
Object 2	1.5	$\begin{bmatrix} 0.015 & 0 & 0 \\ 0 & 0.015 & 0 \\ 0 & 0 & 0.015 \end{bmatrix}$	0.71

Table 2. Time Stamps for tests 1 and 2.

Time Stamp	**Test 1**	**Test 2**
t_1	$10s$	$7.5s$
t_2	$18.5s$	$14.2s$
t_3	$26s$	$22.5s$
t_4	$37.7s$	$32.7s$
t_5	$40s$	$35s$

Table 3 Experimental Results

Operator	$T_{task}\,[s]$	$I_{ev}\,[cm/s]$	$I_{e\omega}\,[rad/seg]$
1	42.3	4.56	0.053
2	71.35	5.13	0.036
3	58.66	9.25	0.016
4	95.71	5.47	0.030
5	48.44	7.03	0.075